The effect of temperature on single-polypeptide adsorption

Sandra Kienle, Susanne Liese, Nadine Schwierz, Roland R. Netz, Thorsten Hugel

Angaben zur Veröffentlichung / Publication details:

Kienle, Sandra, Susanne Liese, Nadine Schwierz, Roland R. Netz, and Thorsten Hugel. 2012. "The effect of temperature on single-polypeptide adsorption." *ChemPhysChem* 13 (4): 982–89. https://doi.org/10.1002/cphc.201100776.

DOI: 10.1002/cphc.201100776

The Effect of Temperature on Single-Polypeptide Adsorption

Sandra Kienle,[a] Susanne Liese,[b] Nadine Schwierz,[b] Roland R. Netz,[b] and Thorsten Hugel*[a]

Dedicated to Professor Christoph Bräuchle on the occasion of his 65th birthday

The hydrophobic attraction (HA) is believed to be one of the main driving forces for protein folding. Understanding its temperature dependence promises a deeper understanding of protein folding. Herein, we present an approach to investigate the HA with a combined experimental and simulation approach, which is complementary to previous studies on the temperature dependence of the solvation of small hydrophobic spherical particles. We determine the temperature dependence of the free-energy change and detachment length upon desorption of single polypeptides from hydrophobic substrates in aqueous environment. Both the atomic force microscopy (AFM) based experiments and the molecular dynamics (MD) simulations show only a weak dependence of the free energy change on temperature. In fact, depending on the substrate, we find a maximum or a minimum in the temperature-dependent free energy change, meaning that the entropy increases or decreases with temperature for different substrates. These observations are in contrast to the solvation of small hydrophobic particles and can be rationalized by a compensation mechanism between the various contributions to the desorption force. On the one hand this is reminiscent of the protein folding process, where large entropic and enthalpic contributions compensate each other to result in a small free energy difference between the folded and unfolded state. On the other hand, the protein folding process shows much stronger temperature dependence, pointing to a fundamental difference between protein folding and adsorption. Nevertheless such temperature dependent single molecule desorption studies open large possibilities to study equilibrium and non-equilibrium processes dominated by the hydrophobic attraction.

1. Introduction

Proteins are main constituents of biological systems and their correct functioning, mainly due to the specific folding behaviour of each single protein, is vital. An important biological question is hence, what forces drive this folding process and how does temperature affect the folding. In the early seventies, Anfinsen studied ribonuclease and showed by unfolding and refolding with urea that the amino acid sequence determines the folding pattern.[1] The fold of a protein can also be changed by varying the temperature. Typical proteins are unfolded (denatured) either by heating them up (heat denaturation)[2] or cooling them down (cold denaturation).[3] This reflects a maximum in the free energy, which can be rationalized by the interplay of opposing contributions to the solvation of hydrophobic residues: the entropic cost decreases with rising temperature while the enthalpic cost goes down as the temperature is lowered.

Despite many efforts to understand and predict protein folding and its temperature dependence,[4] this problem is still unsolved. One reason is that current simulation techniques are too slow for reasonably sized proteins and another that the major contributing forces (which would help for designing approximations) are unclear. The hydrophobic attraction (HA) has long been and is still believed to be one of the main forces in the folding process,[5] but despite decades of research the understanding of the dependence of the HA on key thermodynamic parameters like temperature is still incomplete. Most experimental and theoretical work on HA concentrated on probing the hydration behaviour of small hydrophobic particles and their temperature dependence, which also show a maximum in the free energy.[6] Some of the experiments exhibited entropy convergence, which lend credibility to the idea that HA is the driving force for protein folding (hydrophobic collapse).[7] Although the HA on its own is not sufficient to explain protein structure and stability, it is without doubt an important contribution and worth being studied in detail.

Herein, we investigate the HA from a slightly different perspective compared to previous studies. We determine the free energy necessary to pull a polypeptide from a solid substrate into solution, both with an atomic force microscopy (AFM) based method and with molecular dynamics (MD) simulations. The surfaces used are neither charged nor are they capable of forming hydrogen bonds. Thus, the forces that act between the polypeptides and the surface can only be associated with

[a] S. Kienle, Prof. Dr. T. Hugel
Department of Physics (E22), IMETUM, CeNS
Technische Universität München
Boltzmannstr. 11, 85748 Garching (Germany)
Fax: (+49) 89-289-10805
E-mail: thugel@mytum.de

[b] S. Liese, N. Schwierz, Prof. Dr. R. R. Netz
Fachbereich für Physik, Freie Universität Berlin
Arnimallee 14, 141954 Berlin (Germany)

a hydrophobic attraction. This method allows filling the gap between the solvation of small hydrophobic particles (which was studied in detail before) and larger folded proteins. The experiments were done with a single molecule force sensor that utilizes a single polypeptide covalently attached to an AFM tip. With this sensor, force–distance curves such as depicted in Figure 1 can be obtained at different temperatures. They give information on the mean desorption force (height of the plateau), the detachment length (length of the plateau) and the free energy ΔG of the solvation process. In the past this was done to delineate the influence of the surface[8] and of solutes.[9] Herein, the focus is on the temperature dependence of the desorption process and its relation to the hydrophobic attraction. With one force sensor, several hundred force–distance curves were performed at different temperatures ranging from 299 to 348 K in water. The behaviour of a hydrophilic and a hydrophobic polypeptide were compared on two different surfaces, a hydrogenated diamond and a glass slide which was functionalized with an aminosilane. Both surfaces are hydrophobic but differ slightly in roughness. The results showed that there is only a weak influence of the temperature on the desorption force and on the detachment length and therefore on ΔG. Interestingly, the curvature of the adsorption free energy seems to change sign dependent on surface roughness showing a temperature maximum or a minimum depending on the substrate type. This is in contrast to the solvation of small hydrophobic solutes, where always a maximum in solvation free energy at a specific temperature is found.

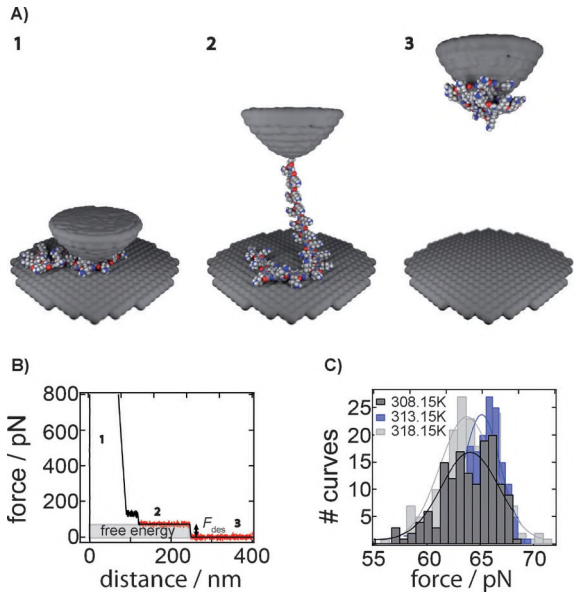

Figure 1. A) Schematic representation of the desorption process of polylysine (not to scale). First, the AFM tip is in contact with the surface to let the polypeptide adsorb (1). Then, the cantilever is retracted and the polypeptide is desorbed from the surface (2) until it is completely detached (3). B) Exemplary force–distance curve of a polylysine chain that was desorbed from a hydrogenated diamond surface. The height of the final plateau corresponds to the desorption force, the area underneath to the free energy and the length to the detachment length (see Experimental and Computational Methods Section for details). C) Exemplary histogram for the desorption forces of three experimental sets for polylysine at different temperatures and corresponding Gaussian fits.

Recently, Horinek et. al showed that MD simulations are capable of describing the desorption of a polypeptide from a solid surface in aqueous environment and to extract molecular details of this process.[10] Therefore, we investigate further details of the desorption process with MD simulations at temperatures between 290 and 430 K. Consistent with the experiments, they show only a weak temperature dependence of the desorption force, with a maximum or minimum depending on the surface type.

2. Results

2.1. Characterization of the Experimental Surface

To investigate the HA, the temperature dependence of the desorption of single hydrophobic and hydrophilic polypeptides from two different hydrophobic surfaces was investigated by means of AFM. The surfaces were a hydrogenated diamond and a glass slide functionalized with an aminosilane. The surface modifications were tested by determining the contact angle with a home-build goniometer equipped with a CCD-camera. For each surface, the angles of five 1.5-µl ultrapure water droplets were recorded and analyzed with a plug-in for the Java-based freeware ImageJ.[11]

With this plug-in, the angles between the surface and the droplets were fitted and determined (see Figure 2 A, right, and Figure 2 B, right). The average contact angles were 75° for the hydrogenated diamond and 83° for the glass slide, respectively. Additionally, AFM contact-mode images (Figure 2 A, left, and Figure 2 B, left) were obtained to compare the mean roughness of the two surfaces. They resulted in a value of 0.6 nm for the diamond and 1.6 nm for the glass slide. An overlay of a line trace for each surface is shown in Figure 2 C. We have two surfaces with similar hydrophobicity, but different chemical composition and a slightly different roughness.

2.2. Temperature-Dependent AFM Measurements

For the temperature-dependent measurements, a polypeptide was covalently bound to the AFM tip. The functionalization of the AFM tip was optimized to have only one or few polypeptides interacting with the surface. We evaluated only experiments with a single detachment at the end of the force–distance trace (see below). Herein, the behaviour of a single hydrophilic polylysine was compared to that of a hydrophobic polytyrosine. For each polypeptide, force–distance curves in a temperature range from room temperature (299 K) to 348 K were recorded. During such a force–distance measurement, the cantilever was lowered until the tip was in contact with the surface. After a dwell time of 1 s, to let the polypeptide adsorb to the surface, the cantilever was retracted with a velocity of 1 $\mu m\,s^{-1}$. During this retraction cycle, the desorption force stays constant until the polypeptide is completely detached from the surface (Figure 1 B). The measured force plateaus are caused by an equilibrium desorption on the timescale of the experiment,[12] which is in contrast to the non-equilibrium rupture forces for covalent bonds.[13] Every single

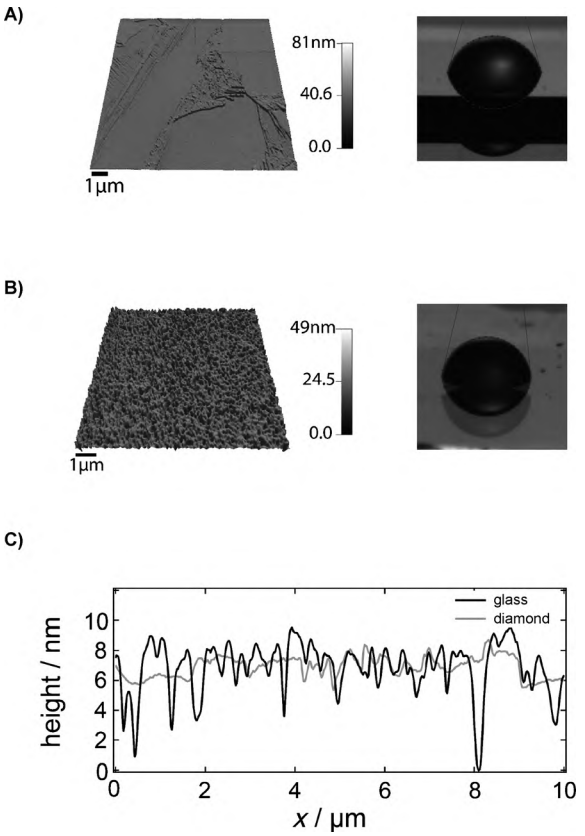

Figure 2. A) Contact-mode image of the hydrogenated diamond (left) and water droplet on the diamond with a fit by ImageJ (right). The resulting average contact angle was 75°. B) Contact-mode images of a glass slide (left) with a contact-angle measurement (right), resulting in an average value for the contact angle of 83°. C) The line profiles for the contact-mode images on glass and diamond show the different roughness of the two surfaces.

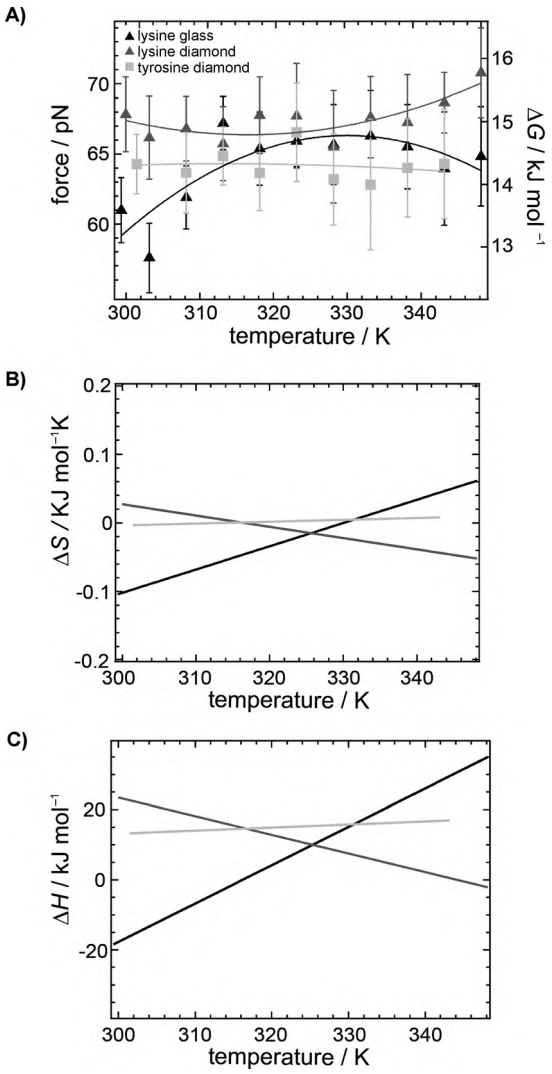

Figure 3. A) Temperature dependence of the desorption force and the desorption free energy per amino acid, ΔG, for polylysine obtained from AFM measurements on the hydrogenated diamond surface (grey triangles) and on the glass slide (black triangles) and for polytyrosine on the hydrogenated diamond (light-grey squares). B) Entropy change per amino acid, ΔS, for the measurements with polylysine on diamond (grey line) and on the glass slide (black line) and with polytyrosine on diamond (light-grey line). C) Enthalpy change per amino acid, ΔH, for polylysine on diamond (grey line) and on the glass slide (black line) and with polytyrosine on diamond (light-grey line). Entropy and enthalpy are determined from a parabolic fit to the free energy.

polymer detaching from the surfaces results in a single step in the force–distance trace.[14] In the exemplary measurement (Figure 1 B), two detachment events can be observed. First, two polypeptides are desorbed in parallel, until the first detaches at a separation of about 120 nm. Then, the second polypeptide is desorbed on its own, until detachment at a separation of about 250 nm from the surface occurs. We only evaluate the desorption force of the polypeptide with a single-step detachment to the baseline (which follows a single-polymer desorption plateau). For each temperature, the force, the length, and the free energy per amino acid, ΔG, for about 100 plateaus, were measured and averaged.

The results for the desorption force and for the desorption free energy per amino acid ΔG are shown in Figure 3 A. Here, the measurement for the hydrophilic polylysine on the diamond substrate shows only weak temperature dependence (grey triangles), with a slight minimum in the free energy. The measurements with polylysine on the glass slide (black triangles) show also a weak dependence, but a slight maximum in the free energy. The larger deviations at low temperatures are still close to the uncertainty of the measurement. The results for the desorption force of polytyrosine on the hydrogenated diamond are also shown in Figure 3 A (light grey squares). Here, neither a minimum nor a maximum can be observed—there is no significant effect of temperature on the desorption free energy.

From these experiments one can also gain information about other thermodynamic parameters, such as the entropy change ΔS and the enthalpy change ΔH (per amino acid), with increasing temperature. Therefore, ΔG was fitted with a parabola for all three data sets. Due to the scatter of the data points, many analytical functions could be fitted—we chose a parabola to compare our results to the solvation free energy of small nonpolar molecules. The fit shows a weak maximum for the measurement with polylysine on glass (which is slightly

rougher than diamond, Figure 2C) and on diamond, a weak minimum. Then, the fits were differentiated to get ΔS and ΔH (see Experimental and Computational Methods Section). The changes in entropy and in enthalpy with temperature are small for polylysine and even negligible for polytyrosine (Figure 3B,C).

2.3 Change of Detachment Length with Temperature

The desorption plateau is in thermodynamic equilibrium on the timescale of the experiment, but the detachment itself is a non-equilibrium process.[12] Therefore, we tested if the detachment length is temperature-dependent. As mentioned before, a plateau with a single detachment to the baseline clearly indicates a single molecule. Although we use the same cantilever for all temperatures in one measurement set (which is necessary to reduce the uncertainties in the desorption force difference), we often lose a cantilever attached polymer and get another one when changing the temperature. For the example shown in Figure 4 we retained the same polymers with the same detachment length for two different temperatures, demonstrating that there is no significant change in detachment length with temperature.

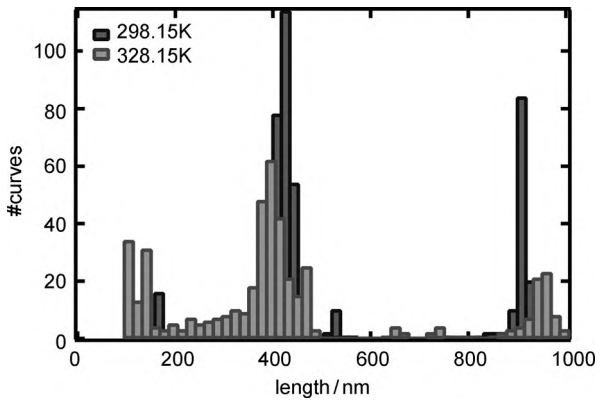

Figure 4. Histogram of the detachment length for polylysine molecules on the hydrogenated diamond for two different temperatures.

2.4. Temperature-Dependent MD Simulations

These experimental results were compared to MD simulations to gain more insight into the details of the desorption process at different temperatures and different substrates. Polylysine exhibited different adsorption behaviors on substrates with different roughness. Due to complicated charge-regulation effects of charged polypeptides at surfaces,[15] polylysine adsorption is not an ideal system for simulations to investigate the HA. For that reason—and to test how universal the experimental results are—we decided to study the simplest peptide in MD simulations, namely, polyglycine. We performed both dynamic and static simulations on two substrates with different roughness. As a surface, a SAM (self-assembled monolayer) or a diamond were used. Their contact angles are 117° and 121° for the SAM and diamond, respectively. In Figure 5, the water density profiles parallel to the surface are shown. Therefore, the simulation box was divided into 200 slices parallel to the *y*–*z* plane. The profile (Figure 5) shows the density as a function of *x*.

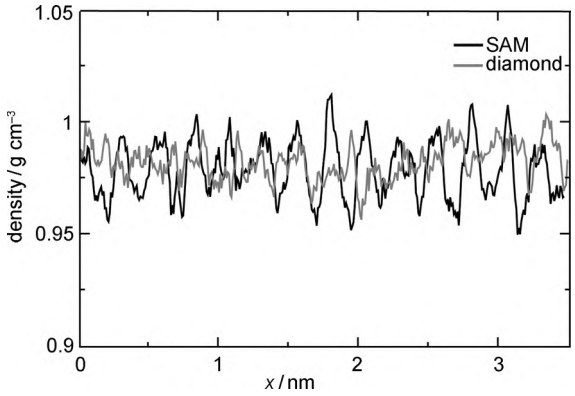

Figure 5. Water density profile parallel to the diamond surface (grey curve) and the SAM (black curve).

As a measure of the roughness, the standard deviation from the mean density was calculated to be 15 mg cm^{-3} on the SAM and 13 mg cm^{-3} on diamond. The density profile on SAM (black curve) exhibits a rough but regular pattern. The density peaks are broadened in comparison to the density profile found on diamond and the peak positions indicate the location of the outermost surface atoms. In contrast, on diamond (grey curve) the density profile is much smoother.

For the dynamic simulations, polyglycine was pushed to a surface. Then, a harmonic potential was applied to the first monomer, so its origin moves away from the surface with a constant velocity of 0.1 m s^{-1}. When the force was strong enough to desorb the peptide, the force–distance curve showed a plateau. After the last monomer was detached, the force dropped to zero. Because the pulling velocity was five orders of magnitude higher than in the AFM experiments, additional static simulations were done to maintain a process close to equilibrium. Here, the potential origin was held at a fixed height. The system configurations were taken from the dynamic simulations and were chosen such that the separation between the surface and the origin of the harmonic potential exhibits a grid of 0.2 nm.

The simulations for polyglycine on a hydrophobic SAM showed only a weak dependence of the desorption force on temperature (Figure 6A, black markers). The same could be seen for simulations on a hydrogenated diamond surface. The desorption force does not change significantly, except for the force at 300 K which is significantly higher than the rest. The simulations are consistent with the experiments. Here, again, the parabolic fit of ΔG results in a weak minimum for diamond and in a weak maximum for the simulations on SAM (which has a larger roughness compared to the diamond). The absolute values for the desorption force are almost a factor of two higher in the experiments. Still, the relative changes in force with temperature matches the experimental data. We next dissect the different contributions to the desorption force:

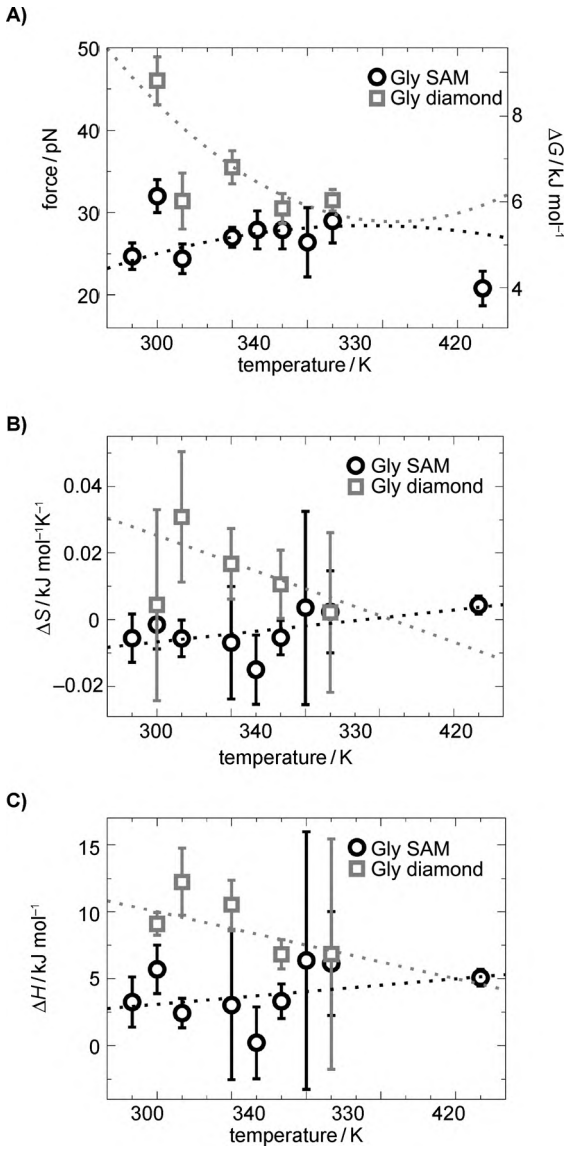

Figure 6. A) Temperature dependence of the desorption force and the desorption free energy per amino acid, ΔG, for polyglycine obtained from MD simulations on the hydrogenated diamond surface (grey markers) and on a SAM (black markers) with a parabolic fit. B) Entropy change per amino acid, ΔS, for the simulations with polyglycine on diamond (grey markers) and on a SAM (black markers). C) Enthalpy change per amino acid, ΔH, for the simulations with polyglycine on diamond (grey markers) and on a SAM (black markers).

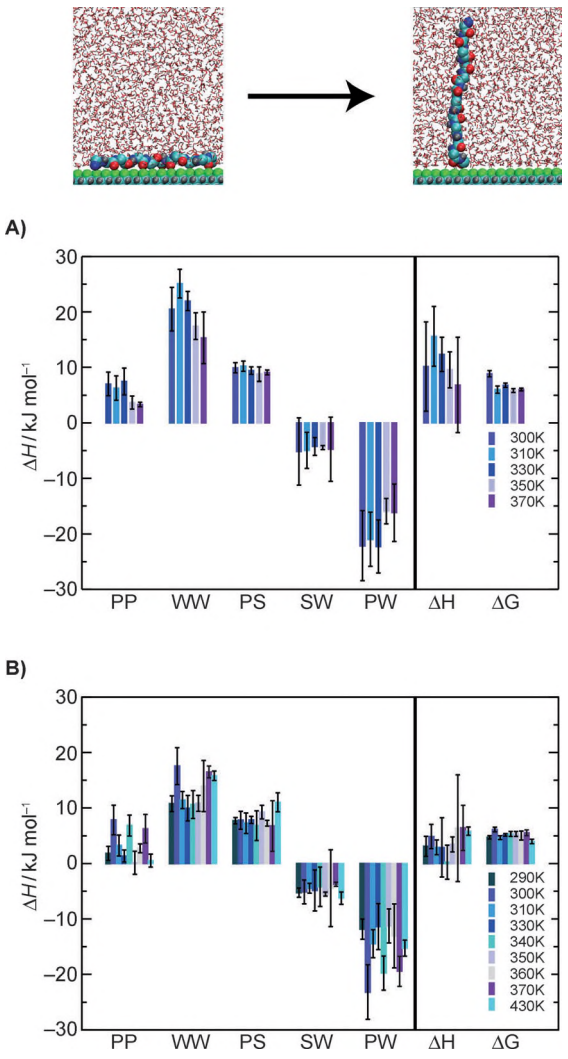

Figure 7. The difference in enthalpy per amino acid at different temperatures is shown between the states where the polypeptide is completely adsorbed and completely stretched on A) diamond and B) SAM as a surface. ΔH can be divided into a sum according to interactions between the contribution from the surface (S), the peptide (P) and the water (W) with one another. The change in free energy, ΔG, is also shown for each temperature.

Figure 7 depicts the differences in enthalpy, ΔH, per amino acid between the states where the polymer is completely adsorbed to the surface and completely stretched (but not detached), respectively. In addition, the interactions between the different components for ΔH in dependence on the temperature are given. Interestingly, the variations in between the different interactions are much larger than the total change in (free) energy. As in the experiments, the temperature dependence of the desorption process is not universal and depends on the details of the peptide–surface interaction.

3. Discussion

Proteins, in general, show a maximum in the folding free energy as a function of the temperature, which characterizes the stability of the native state with respect to the denatured state. Such a maximum was also observed for the solvation of small hydrophobic particles, which is dominated by the HA. For this reason (and additionally enforced by experiments that suggested entropy convergence), the HA was considered the main force controlling the folding of proteins. Herein, we used a new kind of experimental tool to investigate the HA in a geometry that is more complex than the solvation of hydrophobic objects in water, yet simple enough to be studied by solvent-explicit MD simulations. Therefore, a single polypeptide that was attached to an AFM tip was desorbed from a solid substrate at different temperatures. This equilibrium desorption process results in a constant force plateau (Figure 1).

Whatever forces contribute to the interactions between the hydrophobic surface and the hydrophilic or the hydrophobic polypeptides used herein, this force can only be associated with a hydrophobic attraction, since the surfaces in the experiments are neither charged nor are they capable of forming hydrogen bonds.

Despite probing several combinations of polypeptides and surfaces, we only observe a weak dependence of the desorption force on temperature (Figure 3). What can be seen is that for the rougher surface, a weak maximum in desorption free energy was found. On the smoother diamond surface, the fit shows even a slight minimum. The weak temperature effects with maxima or minima (depending on the surface) suggest that the hydrophobic interaction between a polypeptide and a surface is governed by a mechanism different from the solvation of small hydrophobic objects. The latter constitute the standard paradigm for hydrophobic effects in the context of protein folding and always exhibit a maximum in the temperature dependent desorption free energy. The rather strong departure from theoretical expectations suggests studying the simplest peptide in simulations, namely polyglycine, for which aggregation effects (as for polytyrosine) are absent. Indeed, we see similar results as in the experiments, namely a weak temperature effect on desorption force and different curvatures of the desorption free energy as a function of temperature, depending on the substrate used (Figure 6). This can be rationalized by a compensation in between the many different contributions to the desorption force of single polypeptides from solid substrates in aqueous environment (Figure 7). These results show that the desorption process is much more complex than the solvation of simple solutes and depends on the fine structure of the interfacial water structure and the details of the peptide–surface interactions.

The quantities discussed above were determined from equilibrium processes. The detachment process itself is a non-equilibrium process and might therefore show a different behavior with temperature. But the detachment length in our experiments shows no indication for a temperature dependence (Figure 4). This is an important further piece in the puzzle to understand the non-equilibrium detachment process for single polypeptides.

4. Conclusions

The hydrophobic attraction (HA) is one of the main driving forces for protein folding and to unravel its temperature dependence should therefore help understanding the protein folding process. We present a joint experimental and simulation approach to study the HA in a model system that is complementary to the previously studied solvation of small hydrophobic solutes. In AFM-based experiments and MD simulations, we show that polypeptides only exhibit a weak temperature dependence when desorbed from hydrophobic solid substrates (this process is dominated by the HA). In addition, the curvature of the temperature-dependent desorption free energy changes sign depending on the substrate (likely caused by different surface roughness). Unexpectedly, these results differ considerably from studies on the solvation of small hydrophobic solutes, which always exhibit a maximum in the temperature-dependent desorption free energy. Our combined approach can relate this difference to the compensation between the different contributions in the desorption process, which are all larger in magnitude than the final desorption free energy. This is reminiscent of the protein-folding process itself, where large entropic and enthalpic contributions compensate each other to result in a small free-energy difference between the folded and unfolded states. On the other hand, the protein-folding process depends much stronger on the temperature, indicating that neither the solvation of small hydrophobic solutes nor the desorption of polypeptides from solid substrates is sufficient to understand the main driving force for protein folding.

Experimental and Computational Methods

Surface Preparation and Contact-Angle Measurements

Two different hydrophobic surfaces were used for the desorption measurements: A hydrogenated, polycrystalline diamond (Element-Six, Advancing Diamond Ltd., UK) of size 5 mm x 5 mm and a glass slide which was functionalized with an aminosilane (Vectabond™, Axxora, Lörrach, Germany).

For hydrogenation, the polycrystalline diamond was treated following a procedure similar to that published previously.[16] It was first heated in a vacuum chamber up to 700 °C to clean the sample. The hydrogen flow (100 sccm) started with a constant pressure of 10 mbar and was then activated by a microwave plasma reactor (Astex). The diamond was then treated for 15 min at a pressure of 50 mbar. After a soft shut down, the sample was cooled under hydrogen atmosphere (10 mbar, 100 sccm). The hydrogenated diamond was used for several measurements but cleaned before each one by sonicating in acetone and 2-propanol.

The glass slide was first activated in a plasma chamber with oxygen and then rinsed in acetone and functionalized for ten minutes with Vectabond™. Afterwards, the slide was again rinsed with acetone and ultrapure water. It was prepared immediately before the force measurements.

Force Spectroscopy and Imaging by AFM

The measurements were performed with an MFP-3D SA (Asylum Research, Santa Barbara, CA) instrument. A BioHeater™ was used as a closed fluid cell to get a well-defined temperature control. Silicon nitride cantilevers (MLCT) were purchased from Bruker (SPM probes, Camarillo, CA).

A single poly-l-lysine (Sigma Aldrich, 70,000–150,000 Da) or poly-d-tyrosine (Sigma Aldrich, 40,000–100,000 Da) polypeptide was covalently attached via a flexible poly(ethylene-glycol)(PEG)-linker (Rapp Polymere GmbH, Tübingen, Germany) to the AFM tip. Therefore, the cantilevers were first activated in a plasma chamber with oxygen. Afterwards they were dipped in acetone (anhydrous, $\geq$ 99.8 %, VWR) and then incubated for 5 min in a mix of acetone (5 mL) and Vectabond™ (100 µl). After rinsing in acetone and chloroform (anhydrous, $\geq$ 99 %, Sigma Aldrich), the cantilevers were incubated for 45 min in a chloroform-based solution with CH_3O-PEG-NHS (5 kDa) and PEG-α-ω-Di-NHS (6 kDa) (ratio 1:1500). Then, they were rinsed again in chloroform, ethanol (absolute,

> 99.9%, Merck) and borate buffer (pH 8–8.5) before they were put for 1–2 h in the polypeptide solution. Here, both polypeptides were dissolved with a concentration of 2 mg mL^{-1} in the borate buffer. After incubation, the cantilevers were rinsed in TRIS (molecular biology grade, AppliChem, Germany) and ultrapure water (Biochrom, Germany) and then stored in air. All measurements were performed in ultrapure water. Within one experimental data set, the temperatures ranged from 299.35 to 348.15 K and the cantilever was not changed. The experiments were repeated five times. For each temperature, the spring constant of the cantilever had to be determined to calculate the desorption force. This calibration was done with the thermal noise method.[17] Therefore, the inverse optical lever sensitivity (InvOLS) was determined five times before and five times after the measurement. To evaluate one data set with different temperatures the spring constants which were determined for one cantilever at all the different temperatures from power spectrum (which was corrected for temperature) were averaged but not the InvOLS.

For each temperature, about 100 force–distance curves were recorded and analyzed. For a force–distance curve, the cantilever was lowered at a constant velocity (1 μm s^{-1}) until the tip was in contact with the surface. Then, a dwell time of 1 s was applied to let the polypeptide adsorb to the surface. Afterwards the cantilever was retracted with a velocity of 1 μm s^{-1}. During this retraction cycle, the polypeptide was pulled of the surface which resulted in a constant force plateau (Figure 1). The plateaus were fitted with a sigmoidal curve to get the mean desorption force and the length of the force plateau. The obtained forces and lengths were plotted in a histogram. Each data point shown here represents the maximum of a gauss fit to the histogram and the error shown is the standard deviation (SD). The free energies per amino acid, ΔG, were determined by calculating the area under the force curve and dividing by the number of desorbed amino acids (assuming a length of 0.36 nm per amino acid). ΔG was fitted with a parabola (ΔG_{fit}), and then the following equations were used for the calculation of the entropy change ΔS and the enthalpy change ΔH per amino acid [Eqs. (1) and (2)]:

$$\Delta S = -\delta \Delta G_{fit}/\delta T \quad (1)$$

$$\Delta H = T\Delta S + \Delta G \quad (2)$$

To image the surfaces, constant-force-mode measurements were performed using a CSC37 cantilever (MikroMasch, San Jose, CA) in air with a scanrate of 1 Hz. For each image, 512×512 points were recorded. The roughness of the surface was determined by calculating the rms value of the surface height in squares with a side length of 300 nm (roughly in the order of the detachment length). Afterwards the roughness of the single squares was averaged to get the final value for each surface.

MD Simulations

All simulations were carried out with the Gromacs simulation package.[18] The simulation box contained a substrate (diamond or self assembled monolayer), a homopolypeptide and about 2600 SPC/E water molecules. As a peptide, polyglycine with 12 monomers was used, whereby all amino-acid termini were capped to prevent interactions between the charged moieties and the surface.

A double face-centered-cubic lattice with a lattice constant of 0.3567 nm formed the basis of the diamond substrate. The substrate had a height of 1.0701 nm and its (100) surface was oriented parallel to the *x*—*y* plane of the simulation box. The surface was terminated with hydrogen atoms.

The SAM consisted of 7×8 $C_{20}H_{40}$ chains. Their position represents the (111) surface of gold with a lattice constant of 0.5 nm. Each alkane strand was tilted by an angle of 30°. The SAM was terminated with a Lennard-Jones sphere whose interaction parameters were chosen to resemble a hydrophobic surface with a contact angle of 117°. The interaction range σ was set to 0.3748 nm, which displays the interaction range of a CH_3 group and the potential depth was set to 4.711 kJ mol^{-1}. The terminating group did not carry partial charges.

The water density profile parallel to the SAM and the diamond surface was determined (Figure 5) by dividing the simulation box into 200 slices parallel to the *y*—*z* plane. Then, the mean density in each slice over the entire height was calculated over 4 ns. The density profile in Figure 5 shows the density in dependence on *x*. The standard deviation from the mean density was calculated to be 15 mg cm^{-3} on the SAM and 13 mg cm^{-3} on the diamond.

For both substrates, the atom positions were kept fixed during the simulation. For all simulations, a time step of 2 fs was chosen. The temperature was set to values between 290 and 430 K, and a pressure of 1 bar in the *z* direction was applied. For temperature as well as pressure coupling, the Berendsen scheme was used.[19] If not otherwise noticed, all interactions were described by the GROMOS96(53a6) force-field.[20] Bonds containing hydrogen atoms were constrained by LINCS[21] and periodic boundary conditions in all three dimensions in space were applied.

To prepare the dynamic simulation, first an energy minimization was performed for a simulation box containing the substrate, a peptide and water. Afterwards the peptide that was situated about 3 nm above the substrate was pushed with a constant acceleration of 1 nm s^{-12}, which was applied on all atoms, toward the surface. Followed by a 10 ps simulation in an *NVT* ensemble (i.e. at constant particle number, *N*, volume, *V*, and temperature, *T*) and a 5 ns simulation in an NAP_zT ensemble (i.e. at fixed particle number, *N*, surface area, *A*, temperature, *T*, and vertical pressure, P_z). To desorb the peptide from the surface, a harmonic potential was applied to the first monomer. The potential origin was moved perpendicularly away from the surface with a constant velocity of 0.1 m s^{-1}. The desorption force was calculated from the stretching of the harmonic spring and the spring constant of 166 pN nm^{-1}.

The results from the dynamic simulation were used to perform so-called static simulations. For a static simulation, a configuration with a partly desorbed peptide, taken from the trajectory of the pulling simulation, was used as start configuration. The harmonic potential was held at a fixed height over 8 ns. The last 3 ns were evaluated to calculate the desorption force. The error was estimated by block averaging.[22] Ten start configurations were chosen such that a grid of 0.2 nm in pulling height was achieved. Out of the results of these ten simulations the mean desorption force as an average of the single forces was calculated.

To distinguish the contribution from each constituent to the internal energy, reruns of the static simulations were performed. In each rerun, the simulation box contained only one or two of the original constituents, and the interactions between those were determined. A linear regression of the internal energy, *H*, in dependence of the pulling height was performed to calculate the change in *H* between a completely adsorbed and a completely stretched configuration. ΔH can be divided into a sum according to the con-

tributions from the surface (S), the peptide (P) and the water (W), such that $\Delta H = \Delta H_{PP} + \Delta H_{WW} + \Delta H_{PS} + \Delta H_{SW} + \Delta H_{PW}$.

The total error of ΔH is given by [Eq. (3)]:

$$\Delta\Delta H = (\Delta\Delta H^2_{block} + \Delta\Delta H^2_{lin})^{1/2} \quad (3)$$

where $\Delta\Delta H_{block}$ is the mean error of all data points obtained over block averaging and $\Delta\Delta H_{lin}$ is the error of the linear regression. The free energy of adsorption G is defined as the integral of the desorption force over pulling height divided by the number of amino acids. Hence, G and ΔG are given by the product of the force f and Δf, respectively, with the length of the force plateau per amino acid.

The surface tension of the substrate with water was calculated out of the last 4 ns of a 5 ns *NAP$_z$T* simulation. Prior to this, the system was equilibrated by an energy minimization followed by a 10 ps *NVT* relaxation. From the resulting surface tension, γ_{sl}, together with the air–water surface tension of $\gamma_{vl} = 63.2\ mN\,m^{-1}$, determined in a separate simulation, the contact angle was determined by Young's equation for a substrate with fixed atom positions $\cos(\phi) = -\gamma_{sl}/\gamma_{vl}$.

Acknowledgements

Helpful discussions with Michael Geisler, Tobias Pirzer and Felix Sedlmeier, as well as the hydrogenation of the diamonds by Andreas Reitinger, are gratefully acknowledged. Support by the Nanosystems Initiative Munich (NIM) and the German Science Foundation (SFB 863, Hu 997/8–1, NE 810/4-2) is gratefully acknowledged.

Keywords: atomic force microscopy · desorption · molecular dynamics simulations · single-molecule studies · temperature dependence

[1] C. B. Anfinsen, *Science* **1973**, *181*, 223 – 230.
[2] W. Kauzmann, *Adv. Protein Chem.* **1959**, *14*, 1 – 63.
[3] P. L. Privalov, *Crit. Rev. Biochem. Mol. Biol.* **1990**, *25*, 281 – 305.
[4] a) M. Schlierf, M. Rief, *J. Mol. Biol.* **2005**, *354*, 497 – 503; b) M. Oliveberg, Y. J. Tan, A. R. Fersht, *Proc. Natl. Acad. Sci. USA* **1995**, *92*, 8926 – 8929; c) L. Vugmeyster, D. Ostrovsky, *J. Biomol. NMR* **2011**, *50*, 119 – 127; d) A. Gutin, A. Sali, V. Abkevich, M. Karplus, E. I. Shakhnovich, *J. Chem. Phys.* **1998**, *108*, 6466 – 6483; e) D. Chandler, D. M. Huang, *Proc. Natl. Acad. Sci. USA* **2000**, *97*, 8324 – 8327.
[5] K. A. Dill, *Biochemistry* **1990**, *29*, 7133 – 7155.
[6] a) F. Sedlmeier, D. Horinek, R. R. Netz, *J. Chem. Phys.* **2011**, *134*, 055105; b) G. Hummer, S. Garde, A. E. Garcia, M. E. Paulaitis, L. R. Pratt, *Proc. Natl. Acad. Sci. USA* **1998**, *95*, 1552 – 1555.
[7] P. L. Privalov, N. N. Khechinashvili, *J. Mol. Biol.* **1974**, *86*, 665 – 684.
[8] T. Pirzer, T. Hugel, *ChemPhysChem* **2009**, *10*, 2795 – 2799.
[9] M. Geisler, R. R. Netz, T. Hugel, *Angew. Chem.* **2010**, *122*, 4838 – 4841; *Angew. Chem. Int. Ed.* **2010**, *49*, 4730 – 4733.
[10] D. Horinek, A. Serr, M. Geisler, T. Pirzer, U. Slotta, S. Q. Lud, J. A. Garrido, T. Scheibel, T. Hugel, R. R. Netz, *Proc. Natl. Acad. Sci. USA* **2008**, *105*, 2842 – 2847.
[11] A. F. Stalder, G. Kulik, D. Sage, L. Barbieri, P. Hoffmann, *Colloids Surf. A* **2006**, *286*, 92 – 103.
[12] H. J. Kreuzer, D. B. Staple, M. Geisler, T. Hugel, L. Kreplak, *New J. Phys.* **2011**, *13*, 013025.
[13] a) A. Scherer, C. Zhou, J. Michaelis, C. Braeuchle, A. Zumbusch, *Macromolecules* **2005**, *38*, 9821; b) P. Schwaderer, E. Funk, F. Achenbach, J. Weis, C. Brauchle, J. Michaelis, *Langmuir* **2008**, *24*, 1343 – 1349.
[14] M. Geisler, T. Pirzer, C. Ackerschott, S. Lud, J. Garrido, T. Scheibel, T. Hugel, *Langmuir* **2008**, *24*, 1350 – 1355.
[15] R. R. Netz, *J. Phys. Condens. Matter* **2003**, *15*, S239-S244.
[16] M. Dankerl, S. Eick, B. Hofmann, M. Hauf, S. Ingebrandt, A. Offenhausser, M. Stutzmann, J. A. Garrido, *Adv. Funct. Mater.* **2009**, *19*, 2915 – 2923.
[17] T. Pirzer, T. Hugel, *Rev. Sci. Instrum.* **2009**, *80*, 035110.
[18] D. van der Spoel, E. Lindahl, B. Hess, *J. Mol. Model.* **2001**, *7*, 306 – 317.
[19] H. J. C. Berendsen, J. P. M. Postma, W. F. Vangunsteren, A. Dinola, J. R. Haak, *J. Chem. Phys.* **1984**, *81*, 3684 – 3690.
[20] W. F. van Gunsteren, W. R. P. Scott, P. H. Hunenberger, I. G. Tironi, A. E. Mark, S. R. Billeter, J. Fennen, A. E. Torda, T. Huber, P. Kruger, *J. Phys. Chem. A* **1999**, *103*, 3596 – 3607.
[21] T. Darden, D. York, L. Pedersen, *J. Chem. Phys.* **1993**, *98*, 10089 – 10092.
[22] B. Hess, *J. Chem. Phys.* **2002**, *116*, 209 – 217.